Pediatr Surg Int (2010) 26:29–36
DOI 10.1007/s00383-009-2503-y

ORIGINAL ARTICLE

Carbon dioxide modifies the morphology and function of mesothelial cells and facilitates transepithelial neuroblastoma cell migration

Yi Yu · Joachim Kuebler · Stephanie Groos · Martin Metzelder · Silvia Kurpanik · Benno Manfred Ure · Gertrud Vieten

Published online: 22 October 2009

Abstract
Background The response of mesothelial cells to surgical trauma and bacterial contamination is poorly defined. We have recently shown that CO_2 pneumoperitoneum increases systemic metastasis of neuroblastoma cells in a murine model. Thus, we hypothesized that CO_2 alters the morphology and function of mesothelial cells and facilitates transmesothelial tumor cell migration.
Materials and methods Murine mesothelial cells were exposed to 100% CO_2 and 5% CO_2 as control. Scanning electron microscopy (SEM) investigations, as well as LPS-induced granulocyte-colony stimulating factor (G-CSF) production and mitochondrial activity (MTT assay) were measured. Transmesothelial migration of neuroblastoma cells (Neuro2a) was determined using a transwell chamber system.
Results CO_2 incubation was associated with a significant destruction of the microvillar formation in SEM. Migration studies showed that the barrier function of the mesothelial monolayer decreased. A significantly increased migration of neuroblastoma cells was identified after 100% CO_2 exposure ($P < 0.05$). Although the conversion of MTT as an indicator of mitochondrial activity was only slightly and not significantly reduced after CO_2 incubation, the release of G-CSF induced by LPS was completely blocked during the incubation with 100% CO_2 ($P < 0.05$). The capacity of G-CSF release recovered after the incubation.
Conclusion We observed that peritoneal mesothelial cells lose their typical cell morphology by CO_2 incubation, which is accompanied by facilitated migration of neuroblastoma cells. Moreover, the synthesis of immunological factors is blocked, but this effect is not long lasting. These mechanisms may explain an increased metastasis rate of neuroblastoma cells after CO_2 pneumoperitoneum, which was recently observed in a murine model.

Keywords Mesothelial cells · Carbon dioxide · Neuroblastoma · Migration · Cytokines · Scanning electron microscopy

Y. Yu · J. Kuebler · M. Metzelder · S. Kurpanik · B. M. Ure · G. Vieten (✉)
Department of Pediatric Surgery, Hannover Medical School, Carl-Neuberg-Str.1, 30625 Hannover, Germany
e-mail: vieten.gertrud@mh-hannover.de

S. Groos
Department of Cell Biology, Hannover Medical School, Carl-Neuberg-Str.1, 30625 Hannover, Germany

Introduction

Numerous authors have shown that minimally invasive techniques can be used safely and effectively in children with malignant tumors [1–4]. However, the potential impact of CO_2 used for pneumoperitoneum on the behavior and potential progression of malignant tumors remains a matter of discussion. Although some authors reported an increase in cell proliferation and tumor growth [5–8], others found beneficial effects of CO_2 incubation [9, 10].

Most of these investigations were performed using cells from adult tumors, whereas the wide range of pediatric malignancies has been poorly investigated [11]. Neuroblastoma is the most common solid type of cancer in childhood [12, 13] and accounts for approximately 15% of all cancer deaths in young children [14]. We have recently shown that CO_2 pneumoperitoneum increases liver metastasis of peritoneal neuroblastoma in a mouse model [15]. Further in vitro studies mimicked conditions of CO_2

pneumoperitoneum and confirmed a decreased apoptosis and overexpression of the proto-oncogens *c-myc* and *HMGB-1*, which mediate aggressive behavior in neuroblastoma cells [16]. These results pointed to a potentially negative impact and increased malignancy of tumor cells by exposition to CO_2.

The systemic spread of tumor cells depends on the malignant behavior of the specific tumor cells on the one hand, and on the immunological defence mechanisms and blocking capacity of the peritoneal cavity on the other. The barrier function of the abdomen is executed by a specialized epithel, the mesothelium, a single layer of mesodermal origin cells. The specific properties of the peritoneal mesothelial cells are to act as a mechanical barrier with a protective non-adhesive antifriction surface. They alleviate intracoelomic movement, support the local defense and repair reaction by synthesis of cytokines, growth factors and extracellular matrix proteins [17]. For this purpose, mesothelial cells shape an epithelium by cells that adopt predominantly elongated, flattened, and squamous morphology, the boundaries of which are hard to discern [18, 19]. Further characteristic features are the appearance of numerous microvilli and cilia, which densely cover the apical region [20] and different types of intercellular junctions, including tight junctions that bind the cells into an epithelial-like sheet, adherent junctions that attach neighboring cells to each other, and gap junctions that mediate the passage of chemical or electrical signals between cells [21–23].

It was shown in previous animal studies that the reaction of mesothelial cells to different noxa is characterized by bulging and separation of cells, and by exfoliation, resulting in the exposure of submesothelial connective tissue and subsequent infiltration of leukocytes and macrophages within 12–24 h [24]. It was hypothesized that these changes are not agent specific, but rather represent a standardized inflammatory mesothelial response.

We aimed to investigate whether a CO_2 milieu alters the morphology and function of mesothelial cells in vitro and facilitates transmesothelial migration of neuroblastoma cells.

Materials and methods

The research protocol and all animal care procedures were approved by the local government ethics committee (§4/42).

Cell isolation and cell culture

C57BL/6 J mice approximately 4 weeks old were used. They were kept under standard laboratory conditions, i.e. temperature of 23°C, 12 h light/dark cycle and a standard laboratory diet with free access to water and food. The mice were killed by cervical break and the peritoneal cavity was flushed with 20 ml PBS using a 21-gauge needle (Sarstedt, Germany). Thereafter, 5 ml warmed 0.125%/0.05% trypsin/EDTA solution (PAA Laboratories, Pasching, Austria) was injected into the peritoneal cavity and kept for 7 min. The lavage solutions were collected and transferred to a 50-ml centrifuge tube (Sarstedt, Germany) placed on ice. The cells were centrifuged at 1,000 rpm (Heraeus, Hanau, Germany). The pellets were gently re-suspended in fresh RPMI 1640 medium (PAA Laboratories, Pasching, Austria), which included 100 U/ml penicillin (PAA Laboratories, Pasching, Austria), and 100 µg/ml streptomycin (PAA Laboratories, Pasching, Austria), 20% (v/v) heat-inactivated fetal bovine serum (PAA Laboratories, Pasching, Austria), 0.2 I.E. Insulin (Lilly, Bad Homburg, Germany) and 0.5 mg/ml hydrocortisone (Rotexmedica, Trittau, Germany). Cells were cultured in a humidified incubator (Heraeus, Hanau, Germany) with 5% CO_2 at 37°C for 6–8 days until 80–90% confluence occurred. The medium was replaced by fresh medium without hydrocortisone on the second day. Finally, confluent grown cell cultures were used for the experiments. Vitality was checked using trypan blue (Sigma-Aldrich, Taufkirchen, Germany) dye exclusion. The vitality of cells was confirmed to be above 90% throughout the experiments.

The Neuro2a murine neuroblastoma cell line (DSMZ, Braunschweig, Germany) is known for its similarity to human neuroblastoma in biological, physiological and immunological characteristics [25]. Neuro2a cells were cultured in Dulbecco's modified Eagle's medium + 1,000 mg/l glucose + L-glutamine + pyruvate (D-MEM, Gibco Invitrogen, Karlsruhe, Germany) supplemented with 10% (v/v) heat-inactivated fetal bovine serum, 1× non-essential amino acids (Gibco Invitrogen, Karlsruhe, Germany), 100 U/ml penicillin and 100 µg/ml streptomycin. The cultures were split 1:2 once a week using 0.5% trypsin/0.2% EDTA. Cell vitality was checked using trypan blue dye exclusion.

Study design

We determined the optimal number of confluent grown mesothelial cells in preliminary experiments using a 96-well plate (NUNC, Roskilde, Denmark) and 24-well transwell system (Nunc, Roskilde, Denmark). The optimal numbers were 1×10^4 and 2×10^5 cells/well, respectively. The optimal concentration and incubation time of fluorescent dye-Calcein (BD Biosciences, San Jose, CA, USA) for labeling Neuro2a cells were 1 µg/ml and 1 h incubation. Moreover, we identified 2 h as the optimal time

point for determining Neuro2a cell migration. We used lipopolysaccharide (10 μg/ml; LPS, Sigma) to simulate a clinical setting of irritation of the peritoneal cavity and mesothelial cells, respectively.

Scanning electron microscopy

Mesothelial cells were seeded on glass coverslips and cultured until confluency, which was assessed by light microscopy (Leica, Wetzlar, Germany). Gas incubation (5% CO_2 as control and 100% CO_2) was performed as previously described. The samples were fixed in 0.1 M Na–Cacodylate–HCl buffer (pH 7.3) containing 3% glutaraldehyde over night at 4°C. After washing with the fixative buffer, the cells were postfixed in 2% OsO_4 buffered in 0.1 M Na–Cacodylate pH 7.3 for 60 min at room temperature, dehydrated in ascending concentrations of acetone and subsequently dried in a Balzers CPD 030 critical point dryer (Bal-Tec AG, Liechtenstein). The coverslips were mounted on aluminum stubs with conductive plates (Plano, Wetzlar, Germany) sputter coated with gold in a Polaron E 5400 sputter coater (Polaron Equipment Ltd., Watford, UK) and investigated in a scanning electron microscope (SEM) (Philips SEM 505) at an acceleration voltage of 10 kV. Images were recorded using the SEM software version 2.0 [26].

Neuro2a migration assay

Cell migration was assayed using a 10-mm transwell chamber system with 3.0-μm pore polycarbonate filters as previously described [27]. Briefly, 2×10^5 mesothelial cells were applied into the inserts and the chamber systems were preincubated until confluence was confirmed microscopically. The exposition to 5 and 100% CO_2 was performed at atmospheric pressure for 2 h. Following incubation, the inserts were removed into new 24-well plates, adding 500 μl RAW cell supernatant (murine macrophages cell line, DSMZ, Braunschweig, Germany) as chemoattractant or DMEM medium as control into the lower chambers. Calcein-labeled Neuro2a cells (5×10^5 cells/well) were added into each insert and migration occurred during 2 h of incubation in a 5% CO_2–95% air humified incubator. Finally, the cell suspension from each lower chamber was collected and centrifuged at 1,000 rpm at room temperature for 10 min. Cells were re-suspended in 100 μl PBS and the fluorescence was measured at 510/570 nm on a multi-detection reader (Glomax, Promega, Corporation, USA).

MTT assay

Directly and 6 h after gas exposure mitochondrial activity was monitored by the MTT test as previously described [28]. The MTT is a soluble tetrazolium salt [1-(4,5-Dimethylthiazol-2yl)-3,5-diphenylformazan], which is converted in metabolically active cells by the action of a mitochondrial dehydrogenase into an insoluble formazan pigment. The dimension of the resulting crystals correlates with cell activity and incubation time. The color was measured spectrophotometrically (570 nm; Sunrise, Tecan, Switzerland). 10 μl MTT reagent was added to each well and after 4 h incubation under standard conditions, the accumulation of formazan crystals was stopped by adding 100 μl stop solution. The conversion of MTT was determined spectrophotometrically after solubilization of the formazan crystals by incubation overnight at 37°C.

Granulocyte-colony stimulating factor production

Granulocyte-colony stimulating factor (G-CSF) was chosen to measure the impact of CO_2, as it is known to alter the phenotype of neuroblastoma cells [29]. After adding 1×10^4 cells to each well of totally 8 96-well plates, the plates were preincubated in a 5% CO_2–95% air humified incubator at 37°C (NUNC, Roskilde, Denmark) for 3 days until the state of confluence was confirmed microscopically. After preincubation, the medium was changed to a phenol red-free medium (PAA Laboratories, Pasching, Austria). In half of the plates, 10 μg/ml LPS was added for stimulation. Accordingly, 10 μl PBS was added to the control plates. Thereafter, two plates from the stimulation group and two plates from the control group were left at 5% CO_2. The other plates were incubated in a special airtight chamber at 37°C with 100% CO_2 at atmospheric pressure for 4 h. After the gas incubation and 6 h later, their supernatants were collected and stored at −80°C for further ELISA investigations (RD Systems Europe, Ltd, UK).

Statistical analysis

Data were expressed as mean counts ± standard error of the mean (SEM). Data were pooled from at least three independent experiments done in triplicates. The Statistical Package for the Social Sciences was used to analyze data. The results were compared using one-way analysis of variance followed by post hoc analysis for evaluation of differences among the groups. A $P < 0.05$ was considered significant.

Results

Scanning electron microscopy

Scanning electron microscopy (Fig. 1) revealed that under control conditions, the mesothelial cells formed a continuous layer (Fig. 1a). The cells were flat with a slight dome at the nucleus (Fig. 1b, c). Their apical surface was densely

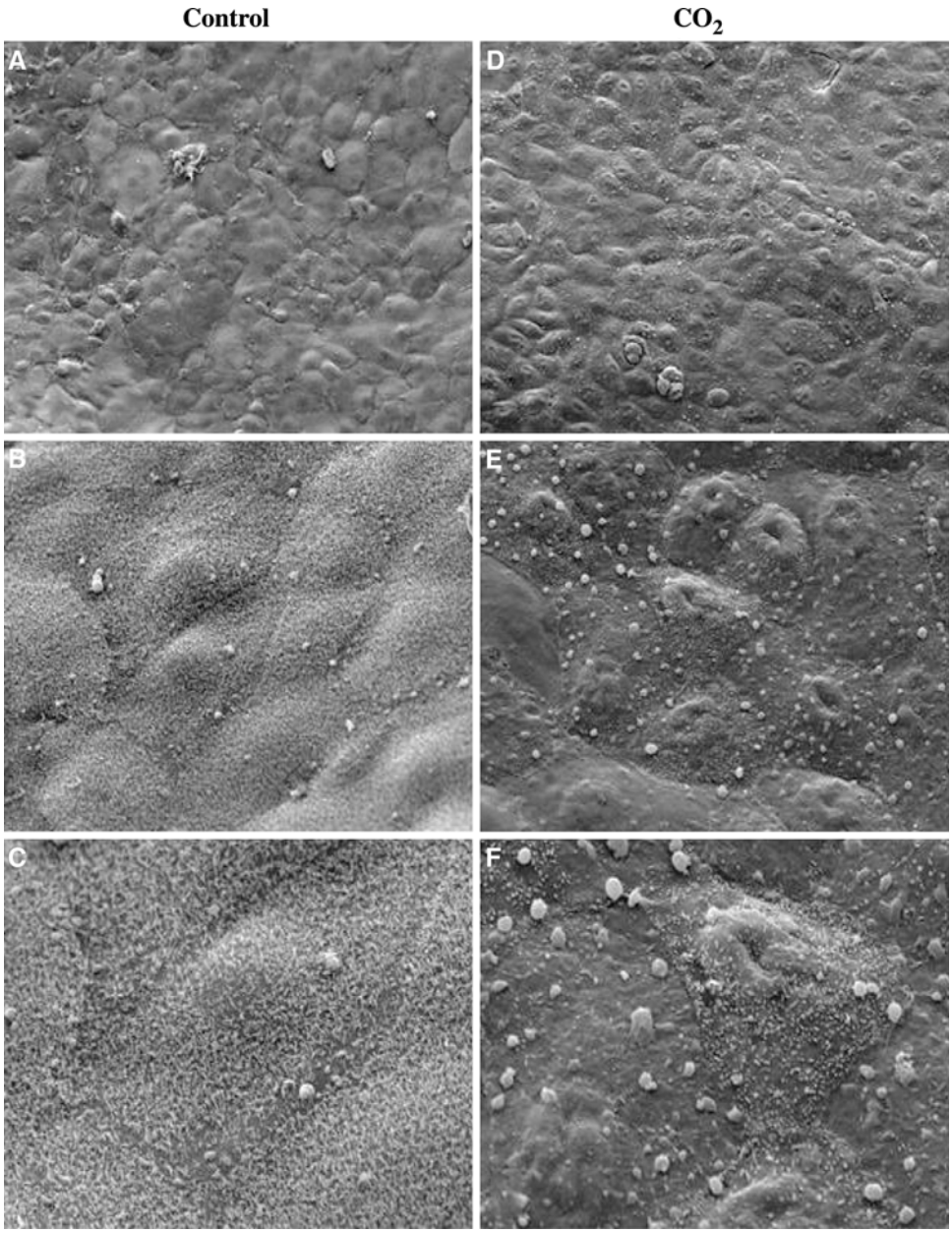

Fig. 1 SEM of mesothelial cell layers. **a–c** Untreated cells, cultured under normal conditions. Confluent mesothelial cell layers were flat with a slight dome at the position of the nucleus. Their apical surface was densely covered by microvilli. **d–f** Mesothelial cells after CO_2 application. Continuous mesothelial cell layers displayed an irregularly shaped dome with a central hollow. The apical cell surface was either devoid of microvilli or their number and length were strongly reduced. Numerous spherical protrusions of the apical membrane could be detected. Magnification **a**, **d** ×300, **b**, **e** ×1,200, **c**, **f** ×2,500

covered by microvilli (Fig. 1b, c). After 4 h of 100% CO_2 the general arrangement of the cells as a continuous layer was unchanged (Fig. 1d). In contrast, the individual cells showed strong alterations of their apical surface (Fig. 1e, f). Most cells displayed an irregularly shaped dome with a central hollow. In addition, the apical cell surface was either devoid of microvilli or their number and length was strongly reduced (Fig. 1e, f). Instead, numerous spherical protrusions of the apical membrane could be detected (Fig. 1e, f).

Migration assay

A significant increase in the chemokine-induced (RAW supernatant) migration of Neuro2a cells was found after 4 h 100% CO_2 incubation compared with 5% CO_2 controls ($P < 0.05$). The fluorescence intensity, which correlates with the number of migrated cells, was 258.56 ± 213.25 in the 100% CO_2 groups. Mesothelial cells cultured under control conditions (5% CO_2) inhibited the migration of Neuro2a (83.67 ± 77.05) (Fig. 2).

Mitochondrial activity

The mitochondrial activity was measured in both groups: the unstimulated control group and the LPS-stimulated group (Fig. 3). Mitochondrial activity in these groups was not significantly different at all time points. However, a mild reductive effect of 100% CO_2 was seen by comparing

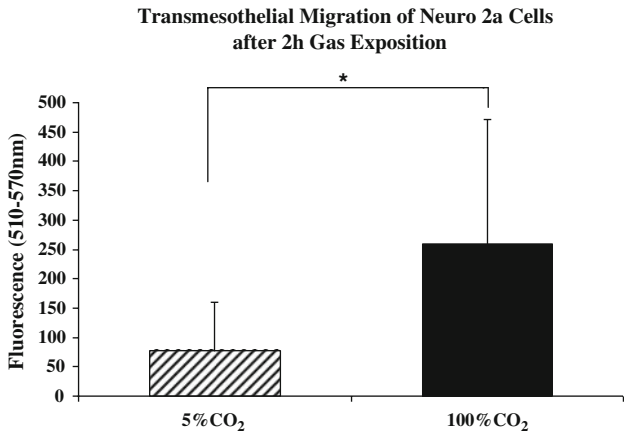

Fig. 2 Impact of 100% CO_2 gas on transmesothelial Neuro2a cell migration. Confluent mesothelial cell layers were exposed to 5% CO_2 or 100% CO_2 for 2 h. Fluorescence-labeled Neuro2a cells were added to the *inserts*. After a further 2 h, tumor cell migration across the monolayer was measured by fluorescence intensity in the lower chamber. The migration was significantly increased in the 100% CO_2 group ($P < 0.05$)

the different gas incubation groups. Directly after the test interval of 4 h, the cells exposed to 5% CO_2 reached activation values of 0.82 ± 0.28 in the unstimulated groups with comparable results in the LPS-stimulated groups 0.82 ± 0.23. The 100% CO_2 groups reached values of 0.57 ± 0.22 (control) and 0.52 ± 0.29 (LPS). After 6 h of incubation, the 5% CO_2 groups reached values of 0.87 ± 0.24 (control) and 0.83 ± 0.36 (LPS) and the values in the 100% CO_2 groups increased somewhat to 0.68 ± 0.28 (control) and 0.70 ± 0.24 (LPS).

G-CSF production

During 4 h of 100% CO_2 exposure, the LPS-stimulated G-CSF production was totally eliminated ($P < 0.05$). During the same time period, mesothelial cells exposed to 5% CO_2 produced 1,047.36 ± 539.38 pg G-CSF/ml. After 6 h of gas exposure, no significant differences could be observed between the 5% CO_2 (1,805.48 ± 404.91 pg G-CSF/ml) and the 100% CO_2 groups, where the growth factor production recovered to 1,064.78 ± 307.54 pg G-CSF/ml ($P > 0.05$). Spontaneous release of G-CSF by mesothelial cells without stimulation (control groups) was not detectable at any time point (Fig. 4).

Discussion

We have recently shown that CO_2 pneumoperitoneum increases systemic metastasis of neuroblastoma cells in a murine model [15]. Therefore, the main focus of the present study was to determine the impact of CO_2 on the functional capacity and morphological integrity of mesothelial cells.

Qualitative SEM investigations demonstrated a homogeneous spreading of numerous microvilli on the apical surface of unaffected mesothelial cell layers. Incubation with 100% CO_2 revealed a significant downregulation of microvillar formation accompanied by an increase in surface-associated vesicles. These results are conclusive with the results of previous investigations done by Volz et al. [30, 31] and Rosário et al [24]. The authors investigated the mesothelium 2 h to 96 h after in vivo CO_2 pneumoperitoneum. Mesothelial cells were bulging upwards and, depending on the duration of incubation increasing intercellular clefts became visible. However, the authors had performed CO_2 pneumoperitoneum using pressure and it remained unclear which of these factors was finally responsible for the effects. Our experiments confirm that CO_2 alone alters the morphological integrity of mesothelial cells.

It is well known that CO_2 exposure of cells and tissue causes hypoxia, and leads to an increased local acidification [32, 33]. Several studies [34–38] have demonstrated that ischemia results in the disruption of the actin-membrane cytoskeleton by activation of an actin depolymerizing

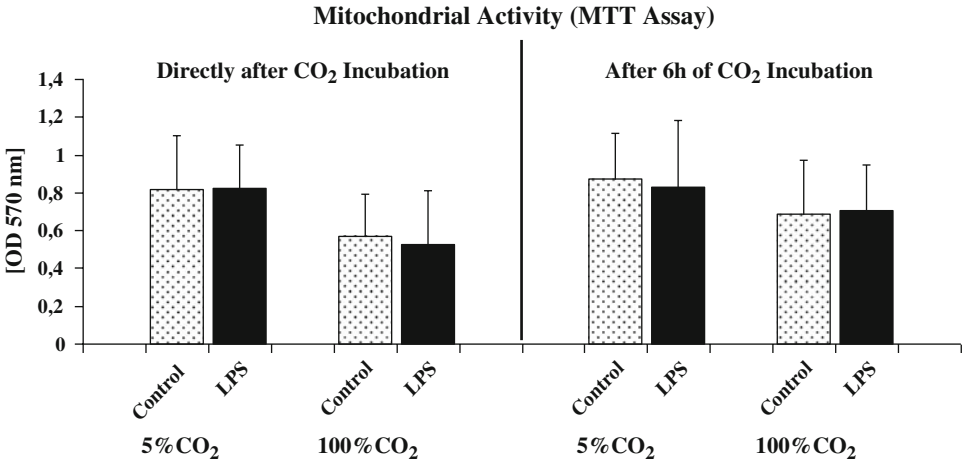

Fig. 3 Mitochondrial activity measured by MTT assay. Incubation of mesothelial cells with 5% CO_2 and 100% CO_2. Activity was measured directly after and 6 h after gas incubation. LPS stimulation was started synchronically with the CO_2 incubation. The reduction in mitochondrial activity after 100% versus 5% CO_2 incubation was not significant. The data were mean ± SEM of three independent investigations

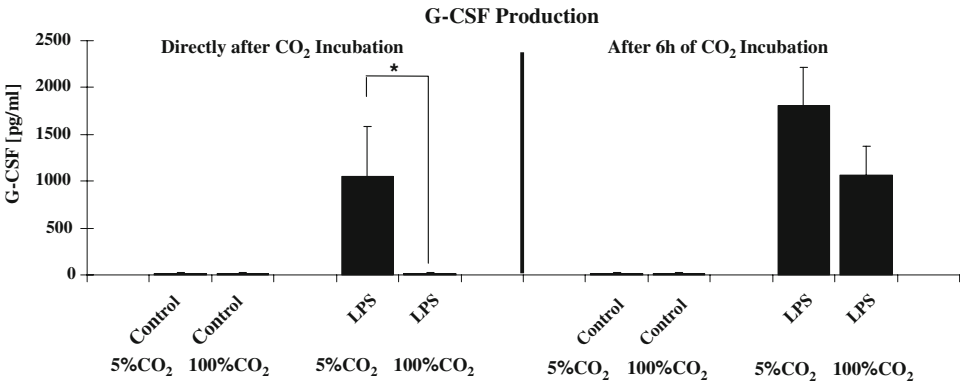

Fig. 4 G-CSF production. Mesothelial cell cultures were divided into control (unstimulated) and LPS-stimulated groups. Synchronically, both groups were exposed to 5% CO_2 and 100% CO_2 for 4 h. G-CSF production was detected directly after incubation and after 6 h. A significant impact of 100% CO_2 was measured directly after gas incubation ($P < 0.05$)

factor. It is also known that extracellular acidification leads to a rearrangement of the cytoskeleton [39]. Our scanning electron microscopic investigations showed a direct alteration of the apical microvilli, which were completely abolished, probably by microvilli retraction into the cells via actin filament disruption. It was not the aim of these examinations to distinguish between effects of hypoxia and acidification causing the ultra-structural alterations in the mesothelial monolayer, but further studies could clarify this question.

It can be speculated that the cell–cell adhesion by tight junctions are also modified. Golenhofen et al. [40] studied various cytoskeletal and functional alterations, such as actin and villin compartmentation using cultured renal cells and observed molecular structural alterations in the tight junctions 60 min after CO_2 exposure. Although we could not detect intercellular clefs in the mesothelial cell monolayer directly after gas exposure by SEM, the decrease in transepithelial resistance would explain the increase in transmesothelial migration of neuroblastoma cells which we determined in the migration assays. Because intercellular clefts show at a later date [30] the loss of cell–cell adhesion must be the first step.

To further study the underlying mechanism of the effects of CO_2 on the metabolism of mesothelial cells, we determined the mitochondrial activity by measuring the redox-equivalent consuming conversion of MTT to its water-insoluble formazan salt. We observed a temporary slight decrease in mitochondrial activity during CO_2 incubation. However, in contrast to our studies on peritoneal macrophages and tumor cells [16, 32, 41], the measured decrease in mitochondrial activity during CO_2 incubation was not significant in our experiments.

It has been postulated that minimally invasive techniques, and in particular the use of CO_2 for pneumoperitoneum, may have an impact on the behavior of the peritoneal immune system. In vivo and in vitro studies have demonstrated that CO_2 can modify oxidative stress markers after laparoscopic operations [41–45]. In vitro studies on neutrophils and macrophages [27, 32, 33] showed a direct and temporary suppression of proinflammatory cytokines. So far, the effect of 100% CO_2 on the cytokine production of mesothelial cells has not been investigated. Focused on the synthesis of G-CSF, a significant inhibition of the production during 100% CO_2 exposure was documented. As observed by us, the effect is temporary, but the results show the importance of the mesothelium for the local immune response of the peritoneum. Further investigation is needed on the immunomodulatory aspects of the mesothelial cell compartment.

Although the observed effects cannot be transferred one by one to the in vivo situation, our investigations confirm specific effects of CO_2 on mesothelial cells. We observed an increased transmesothelial migration of neuroblastoma cells with CO_2 incubation-associated alteration of the mesothelial cytoskeleton. Another CO_2 induced effect to mesothelial cells was a temporary reduction in the cell metabolism, which was monitored by a decrease in mitochondrial activity and significant suppressed cytokine production. These effects may support the hypothesis of the role of the mesothelial cell in an increased migration of cancer cells during and after pneumoperitoneum. The role of mesothelial cells play in this context now remains to be determined in vivo.

Acknowledgments The authors thank Mrs. Renate Schottmann and Mrs. Birgit Teichmann for their excellent technical assistance. The authors also thank Mrs. Clare Boerner for her editorial assistance.

References

1. Metzelder ML, Kuebler JF, Shimotakahara A, Glueer S, Grigull L, Ure BM (2007) Role of diagnostic and ablative minimally invasive surgery for pediatric malignancies. Cancer 109:2343–2348
2. Iwanaka T, Kawashima H, Uchida H (2007) The laparoscopic approach of neuroblastoma. Semin Pediatr Surg 16:259–265
3. Leclair MD, de Lagausie P, Becmeur F, Varlet F, Thomas C, Valla JS, Petit T, Philippe-Chomette P, Mure PY, Sarnacki S, Michon J, Heloury Y (2008) Laparoscopic resection of abdominal neuroblastoma. Ann Surg Oncol 15:117–124

4. Chan KW, Lee KH, Tam YH, Yeung CK (2007) Minimal invasive surgery in pediatric solid tumors. J Laparoendosc Adv Surg Tech A 17:817–820
5. Jacobi CA, Wenger F, Sabat R, Volk T, Ordemann J, Müller JM (1998) The impact of laparoscopy with carbon dioxide versus helium on immunologic function and tumor growth in a rat model. Dig Surg 15:110–116
6. Cirocco WC, Schwartzman A, Golub RW (1994) Abdominal wall recurrence after laparoscopic colectomy for colon cancer. Surgery 116:842–846
7. Gleeson NC, Nicosia SV, Mark JE, Hoffman MS, Cavanagh D (1993) Abdominal wall metastases from ovarian cancer after laparoscopy. Am J Obstet Gynecol 169:522–523
8. Muntz HG, Goff BA, Madsen BL, Yon JL (1999) Port site recurrence after laparoscopic surgery for endometrial carcinoma. Obstet Gynecol 93:807–809
9. Are C, Talamini MA (2005) Laparoscopy and malignancy. J Laparoendosc Adv Surg Tech A 15:38–47
10. Bouvy ND, Marquet RL, Hamming JF, Jeekel J, Bonjer HJ (1996) Laparoscopic surgery in the rat: beneficial effect on body weight and tumor take. Surg Endosc 10:490–494
11. Iwanaka T, Arya G, Ziegler MM (1998) Mechanism and prevention of port-site tumor recurrence after laparoscopy in a murine model. J Pediatr Surg 33:457–461
12. Maris JM, Hogarty MD, Bagatell R, Cohn SL (2007) Neuroblastoma. Lancet 369:2106–2120
13. Suita S, Tajiri T, Higashi M, Tanaka S, Kinoshita Y, Takahashi Y, Tatsuta K (2007) Insights into infant neuroblastomas based on an analysis of neuroblastoma detected by mass screening at 6 months of age in Japan. Eur J Pediatr Surg 17:23–28
14. George RE, Sanda T, Hanna M, Fröhling S, Luther W 2nd, Zhang J, Ahn Y, Zhou W, London WB, McGrady P, Xue L, Zozulya S, Gregor VE, Webb TR, Gray NS, Gilliland DG, Diller L, Greulich H, Morris SW, Meyerson M, Look AT (2008) Activating mutations in ALK provide a therapeutic target in neuroblastoma. Nature 455:975–978
15. Metzelder M, Kuebler J, Shimotakahara A, Vieten G, von Wasielewski R, Ure BM (2008) CO(2) pneumoperitoneum increases systemic but not local tumor spread after intraperitoneal murine neuroblastoma spillage in mice. Surg Endosc 22:2648–2653 [Epub 13 Feb 2008]
16. Reismann M, Wehrmann F, Schukfeh N, Kuebler JF, Ure B, Glüer S (2009) Carbon dioxide, hypoxia and low PH lead to overexpression of c-mys and HMGB-1 oncogenes in neuroblastoma cells. Eur J Pediatr Surg 19:224–227 [Epub 22 Apr 2009]
17. Yung S, Chan TM (2007) Mesothelial cells. Perit Dial Int 27 Suppl 2:S110–S115
18. Mutsaers SE (2002) Mesothelial cells: their structure, function and role in serosal repair. Respirology 7:171–191
19. Kimura A, Koga S, Kudoh H, Iitsuka Y (1985) Peritoneal mesothelial cell injury factors in rat cancerous ascites. Cancer Res 45:4330–4333
20. Ordemann J, Jakob J, Braumann C, Kilian M, Bachmann S, Jacobi CA (2004) Morphology of the rat peritoneum after carbon dioxide and helium pneumoperitoneum: a scanning electron microscopic study. Surg Endosc 18:1389–1393 [Epub 15 Jul 2004]
21. Thuijls G, de Haan JJ, Derikx JP, Daissormont I, Hadfoune M, Heineman E, Buurman WA (2009) Intestinal cytoskeleton degradation precedes tight junction loss following hemorrhagic shock. Shock 31(2):164–169
22. Tsukita S, Furuse M, Itoh M (2001) Multifunctional strands in tight junctions. Nat Rev Mol Cell Biol 2:285–293
23. Fleming S (1991) C. L. Oakley Lecture (1991). Cell adhesion and epithelial differentiation. J Pathol 164:95–100
24. Rosário MT, Ribeiro U Jr, Corbett CE, Ozaki AC, Bresciani CC, Zilberstein B, Gama-Rodrigues JJ (2006) Does CO_2 pneumoperitoneum alter the ultra-structure of the mesothelium? J Surg Res 133:84–88 [Epub 19 Dec 2005]
25. Ziegler MM, Ishizu H, Nagabuchi E, Takada N, Arya G (1997) A comparative review of the immunology of murine neuroblastoma and human neuroblastoma. Cancer 79:1757–1766
26. Gebert A, Preiss G (1998) A simple method for the acquisition of high-quality digital images from analog scanning electron microscopes. J Microsc 191:297–302
27. Shimotakahara A, Kuebler JF, Vieten G, Kos M, Metzelder ML, Ure BM (2008) Carbon dioxide directly suppresses spontaneous migration, chemotaxis, and free radical production of human neutrophils. Surg Endosc 22:1813–1817 [Epub 11 Dec 2007]
28. Gerlier D, Thomasset N (1986) Use of MTT colorimetric assay to measure cell activation. J Immunol Methods 94:57–63
29. Gay AN, Chang S, Rutland L, Yu L, Byeseda S, Naik-Mathuria B, Cass DL, Russell H, Olutoye OO (2008) Granulocyte colony stimulating factor alters the phenotype of neuroblastoma cells: implications for disease-free survival of high-risk patients. J Pediatr Surg 43:837–842
30. Volz J, Köster S, Spacek Z, Paweletz N (1999) Characteristic alterations of the peritoneum after carbon dioxide pneumoperitoneum. Surg Endosc 13:611–614
31. Volz J, Köster S, Spacek Z, Paweletz N (1999) The influence of pneumoperitoneum used in laparoscopic surgery on an intraabdominal tumor growth. Cancer 86:770–774
32. Kuebler JF, Kos M, Jesch NK, Metzelder ML, van der Zee DC, Bax KM, Vieten G, Ure BM (2007) Carbon dioxide suppresses macrophage superoxide anion production independent of extracellular pH and mitochondrial activity. J Pediatr Surg 42:244–248
33. Kos M, Kuebler JF, Jesch NK, Vieten G, Bax NM, van der Zee DC, Busche R, Ure BM (2006) Carbon dioxide differentially affects the cytokine release of macrophage subpopulations exclusively via alteration of extracellular pH. Surg Endosc 20:570–576 [Epub 25 Jan 2006]
34. Schwartz N, Hosford M, Sandoval RM, Wagner MC, Atkinson SJ, Bamburg J, Molitoris BA (1999) Ischemia activates actin depolymerizing factor: role in proximal tubule microvillar actin alterations. Am J Physiol 276:F544–F551
35. Kellerman PS, Boqusky RT (1992) Microfilament disruption occurs very early in ischemic proximal tubule cell injury. Kidney Int 42:896–902
36. Kellerman PS, Clark RA, Hoilien CA, Linas SL, Molitoris BA (1990) Role of microfilaments in the maintenance of proximal tubule structural and functional integrity. Am J Physiol 259:F279–F285
37. Molitoris BA (1991) Ischemia-induced loss of epithelial polarity: potential role of the actin cytoskeleton. Am J Physiol 260:F769–F778
38. Molitoris BA (1997) Putting the actin cytoskeleton into perspective: pathophysiology of ischemic alterations. Am J Physiol 272:F430–F433
39. Faff L, Nolte C (2000) Extracellular acidification decreases the basal motility of cultured mouse microglia via the rearrangement of the actin cytoskeleton. Brain Res 853:22–31
40. Golenhofen N, Doctor RB, Bacallao R, Mandel LJ (1995) Actin and villin compartmentation during ATP depletion and recovery in renal cultured cells. Kidney Int 48:1837–1845
41. Jesch NK, Kuebler JF, Nguyen H, Nave H, Bottlaender M, Teichmann B, Braun A, Vieten G, Ure BM (2006) Laparoscopy vs. minilaparotomy and full laparotomy preserves circulatory but not peritoneal and pulmonary immune responses. J Pediatr Surg 41:1085–1092
42. Polat C, Kahraman A, Yilmaz S, Koken T, Serteser M, Akbulut G, Arikan Y, Dilek ON, Gokce O (2003) A comparison of the

oxidative stress response and antioxidant capacity of open and laparoscopic hernia repairs. J Laparoendosc Adv Surg Tech A 13:167–173
43. Gál I, Róth E, Lantos J, Varga G, Jaberansari MT (1997) Inflammatory mediators and surgical trauma regarding laparoscopic access: free radical mediated reactions. Acta Chir Hung 36:97–99
44. Seven R, Seven A, Erbil Y, Mercan S, Burçak G (1999) Lipid peroxidation and antioxidant state after laparoscopic and open cholecystectomy. Eur J Surg 165:871–874
45. Glantzounis GK, Tselepis AD, Tambaki AP, Trikalinos TA, Manataki AD, Galaris DA, Tsimoyiannis EC, Kappas AM (2001) Laparoscopic surgery-induced changes in oxidative stress markers in human plasma. Surg Endosc 15:1315–1319 [Epub 16 Aug 2001]